Soils and Rocks
An International Journal of Geotechnical and Geoenvironmental Engineering
www.soilsandrocks.com
ISSN 1980-9743
ISSN-e 2675-5475

Interpretation of large diameter preliminary pile tests in Ampthill Clay, West Walton and Oxford Clay formations for Thame Valley Viaduct

Sergio Vitorino[1#], Hoe-Chian Yeow[2]

Article

Keywords
Pile
Test pile
Back analysis
Plaxis
Osterberg cell

Abstract

Two instrumented preliminary test piles have been installed and tested in Aylesbury, UK, using Osterberg Cell bi-directional load test method, for the purpose of verifying the construction methodology and load performance of the bored piled foundations designed for the 880m long HS2 Thame Valley Viaduct. The local ground conditions comprise stiff clay and mudstone of Ampthill Clay, West Walton and Oxford Clay Formations which constitute part of the Ancholme Group. The significant length of the asset allowed a comprehensive ground investigation package of site and laboratory testing to be undertaken in developing a refined detailed design in accordance with the recommendations of Eurocode 7. The field test results of the two test piles have been interpreted and back-analysed using 3D finite element analyses undertaken to simulate the bi-directional loading of the Osterberg Cell testing method and compared against the ultimate pile capacity estimated during detailed design of the viaduct. Subsequent simulation of the pile loaded from pile head level using the calibrated finite element model provided the required load-settlement characteristic necessary to verify the performance of the pile under serviceability limit state.

1. Introduction

High Speed 2 (HS2) is a high-speed line under construction in England, connecting London to the West Midlands (Phase 1) through approximately 230 kilometres (km) of railway. HS2 Contract C23 (formally Central Area 2 and Central Area 3) covers 80km of railway between North Portal of Chiltern Tunnel (southern end) and the South Portal of Itchington Wood Green Tunnel (northern end). It covers four major geological groups and thirteen geological formations; from the White Chalk Group at the southern end to Ancholmer Group, Great Oolite Group and Lias Group to the north. Five sets of preliminary test piles were installed and tested in the five geological groups to verify pile design assumptions made for piled foundations along the route. Table 1 summarises the eleven (11) preliminary test piles for the C23 HS2 project between September 2020 and August 2021.

Figure 1 shows approximate locations of the preliminary test piles for the HS2 project.

Two preliminary test piles (PTP10A and PTP11) were installed and tested using bi-directional Osterberg Load Cell (O-cell) at the 880m long Thame Valley Viaduct (TVV), as part of the Aylesbury Area package of the HS2 project. These test piles were found in the local ground conditions comprising Ampthill Clay (AMC), West Walton Formation (WWB) and Oxford Clay (OXC). The Arcadis, Setec, COWI Design Joint Venture (ASC) has been appointed by Eiffage, Kier, Ferrovial, and BAM Nuttall Joint Venture to provide detailed design services for the civil engineering assets within HS2. Bauer Keller joint venture (BKJV) was responsible for the installation of the piles while Fugro Loadtest was responsible for testing the piles.

Due to access and programme constraints, the test site was located approximately 200m north of the viaduct's proposed north abutment.

O-cell has transformed pile load test since its invention in the mid-1980s by Dr Jorj O. Osterberg (Hayes, 2012). This method of testing pile has several advantages over conventional pile test methods, including the elimination of the need for a reaction frame or kentledge. O-cell testing method was selected for the HS2 project primarily due to its capability to safely apply very high test loads to full-size test piles. This is achieved by embedding hydraulic jacks within the pile shaft with the reaction to the applied load provided by the ground itself, without the need to handle the heavy reaction system in the form of structural steel frame or concrete kentledge blocked to provide the resistance to the applied load. Furthermore, in the event of any unforeseen failure of

#Corresponding author. E-mail address: s.vitorino@rendel-ltd.com
[1]Rendel Ltd., London, United Kingdom.
[2]COWI UK Ltd., London, United Kingdom.

Submitted on February 12, 2025; Final Acceptance on September 27, 2025; Discussion open until February 28, 2026.
Editor: Renato P. Cunha
https://doi.org/10.28927/SR.2025.002825

Table 1. Preliminary test piles for the C23 HS2 project.

Test pile	Geological Formation	Date tested	Pile length (m)	Diameter (mm)	Maximum test load (MN)[1]
PTP1	Chalk	18/10/21	39.7	1500	21.0
PTP2		25/10/21	35.7	2000	17.7
PTP3	Oxford Clay	08/12/20	40.1	1200	7.7
PTP4		14/12/20	40.5	1200	7.7
PTP5	Charmouth Mudstone	28/09/20	20.8	1500	5.3
PTP6		05/10/20	20.9	1500	6.4
PTP8		09/10/20	26.0	900	6.2/9.32[2]
PTP9		19/10/20	26.0	900	6.5/9.72[2]
PTP10A	Ampthill Clay, West Walton and Oxford Clay	17/03/22	41.1	1500	11.5
PTP11		09/03/22	39.1	1800	24.2

[1]Maximum load applied by O-cell during test (total load is two times O-cell load). [2]Maximum load applied to top/bottom O-cell.

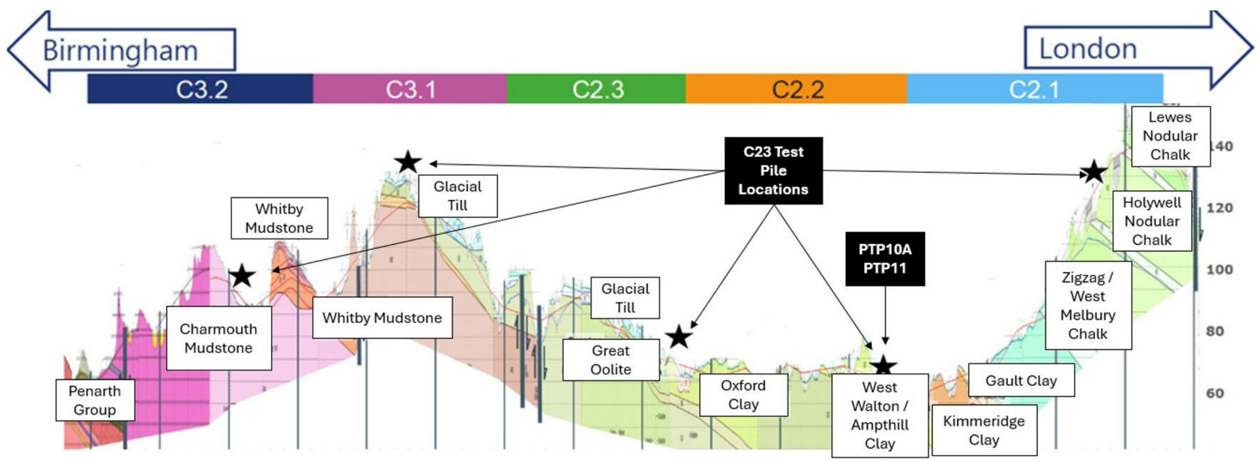

Figure 1. Approximate locations of the preliminary test piles of HS2 project.

the reaction system, the O-cell test method would only need to cater for more manageable burst hydraulic hose while such event, when occur in conventional pile test methods, could lead to a catastrophic collapse of the steel reaction frame or kentledge assembly. Compared to conventional top loaded test pile using kentledge or reaction frame system, any test load beyond 30MN would be very expensive to perform, if not impossible, whereas O-cell test method could achieve a maximum test load well beyond 300MN. As the need to limit the test load in construction industry prior to the use of O-cell, conventional test piles would be performed on smaller size piles and the test data is then used directly for larger size working piles. The use of O-cell to test full size piles would eliminate the uncertainty of scaling the test data from small diameter test pile to a larger working pile. This includes the effects of construction of full-size pile when using O-cell to test the pile.

Testing pile using O-cell is not without its disadvantages. As the O-cell test applies load bidirectionally with sacrificial load cell(s) cast into the pile shaft unless the test pile is founded in rock or similar ground with very high end bearing capacity, determining the most appropriate position of the load cell(s) in the pile is critical to maximise the load applied. Any failure of the pile upwards or downwards before achieving the intended load due to incorrect positioning of the cell means premature end of the test. This is possibly the main disadvantage of using such testing method. Another disadvantage is the more complex installation process involving tremie concrete placement over the full length of the pile with the O-cell positioned at some distance above the pile toe. As the load is applied directionally, it is impossible to accurately determine the portion of the mobilized shaft and base resistance to an equivalent load when applied directly from the pile head under normal pile loading situation. This prevents an accurate determination of the magnitude of load holding for maintained load test commonly specified for static load test under the Institution of Civil Engineers' specification for load test (ICE, 2017). As a direct consequence of such limitation, the interpretation of the load-settlement performance of the test pile is also more complex without resolving to full calibration using more advance numerical modelling.

There is very sparse case history information available on pile performance in the local ground conditions of the TVV site. These tests were deemed necessary to fill the knowledge gap of the designers of the HS2 project and this paper presents the interpretation and back-analysis of the test data with the objective of verifying the design approach adopted for the design of the viaduct piled foundations and the performance of the pile under serviceability limit state. It also provides a comparison of the methods of deriving the test pile's load-settlement performance required for pile tested using O-cell.

2. The site

2.1 Geological setting

Aylesbury Area is situated in the East Midlands Shelf which contains an Ancholme Group succession of clay and mudstone formation which were deposited in the Upper Jurassic period. The ground conditions at the test site are consistent with the ground conditions along the viaduct and comprise less than 1m of Head Deposits (HEAD) overlying AMC, WWB and OXC to depth greater than 60m. AMC and WWB are generally described as stiff to very stiff Clays or calcareous Clays, with small localised pockets of siltstone and limestone, while OXC is generally described as extremely weak Mudstone.

2.2 Site investigation and soil parameters

The ground conditions at the test site have been characterised based on ground investigation works within a 200m radius, which include 6 No. Cone Penetration Tests (CPT), 11 No. boreholes, 6 No. trial pits and respective in-situ and laboratory tests (see Figure 2). The borehole descriptions at the test site and along with the viaduct are not always consistent which could imply a very significant variation in the thicknesses of AMC and WWB, even in boreholes located adjacent to each other. This possibly highlights the difficulty in identifying the marker horizons that distinguish AMC, WWB and OXC, therefore resulting in very different stratigraphy being presented in adjacent boreholes. Despite the discrepancies noted above, the analysis of the Atterberg limits suggests a relatively flat stratigraphy throughout the northern section of the viaduct and the pile test site. Other markers such as calcareous siltstone, thinly interbedded limestone and limestone bands present in AMC and WWB formations also support an assumption of horizontal stratigraphy or otherwise a slight dip towards the south, which would be expected following the general trend of the geology in Aylesbury Area.

Figure 3 presents undrained shear strength and Atterberg limits versus elevation while considering the site ground investigation data. Borehole ML065-CR532A has been drilled at the test site.

The undrained shear strength profile has been determined based on in-situ and laboratory tests.

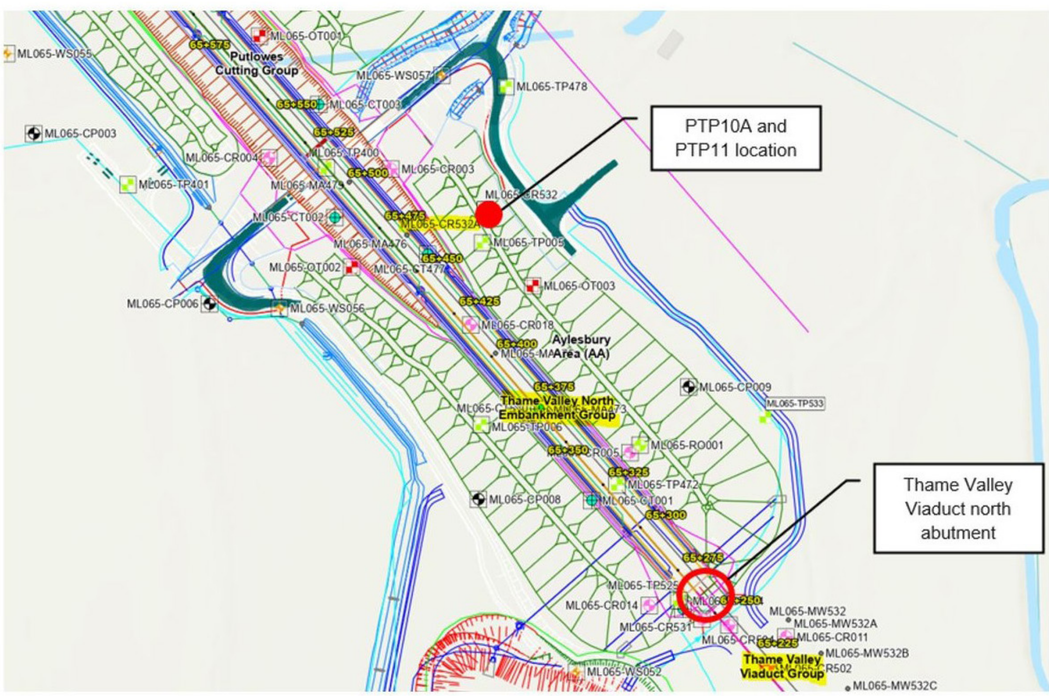

Figure 2. Location plan of the two preliminary test piles PTP10A and PTP11, approximately 200 m north of the viaduct's proposed north abutment.

- Where estimated from CPT, $c_u = (q_c - \sigma_v)/N_{kt}$ with N_{kt} assumed as 17.
- Where estimated from Standard Penetration Tests (SPT), $c_u = f_1 N_{60}$ as proposed in (Clayton, 1995) where $f_1 = 4.5$, based on plasticity index for most of the layers except WWB. For WWB f_1 has been taken as 6 for better fit with the triaxial (TRX) test data.
- Where estimated from Uniaxial Compressive Strength tests (UCS), undrained shear strength was taken as $c_u = UCS/2$.
- The design profile of the test pile has been developed based on the characteristic undrained shear strength profile shown as continuous black line in Figure 3.

Table 2 summarises the stratigraphy and the key geotechnical parameters considered at the test site. AMC has been split into AMC I and AMC II to reflect a change in the plasticity index below 58m AOD (m Above Ordnance Datum), with a slight adjustment in the undrained shear strength profile. The equivalent undrained shear strength of the OXC has been determined using the *UCS* values from laboratory tests of an extremely weak mudstone.

3. Viaduct and pile design

3.1 Description of the viaduct and the foundations

The viaduct carries HS2 over the Thame Valley flood plain, a relatively flat area of open fields surrounding the Thame River which runs approximately North East to South West across the proposed route.

Thame Valley Viaduct is a 36 span, 880m long continuous structure consisting of 4 No. 20 m long spans and 32 No. 25 m long spans. The piers are connected to 12x2.5x1.8 m deep pile caps which are in turn supported by a single

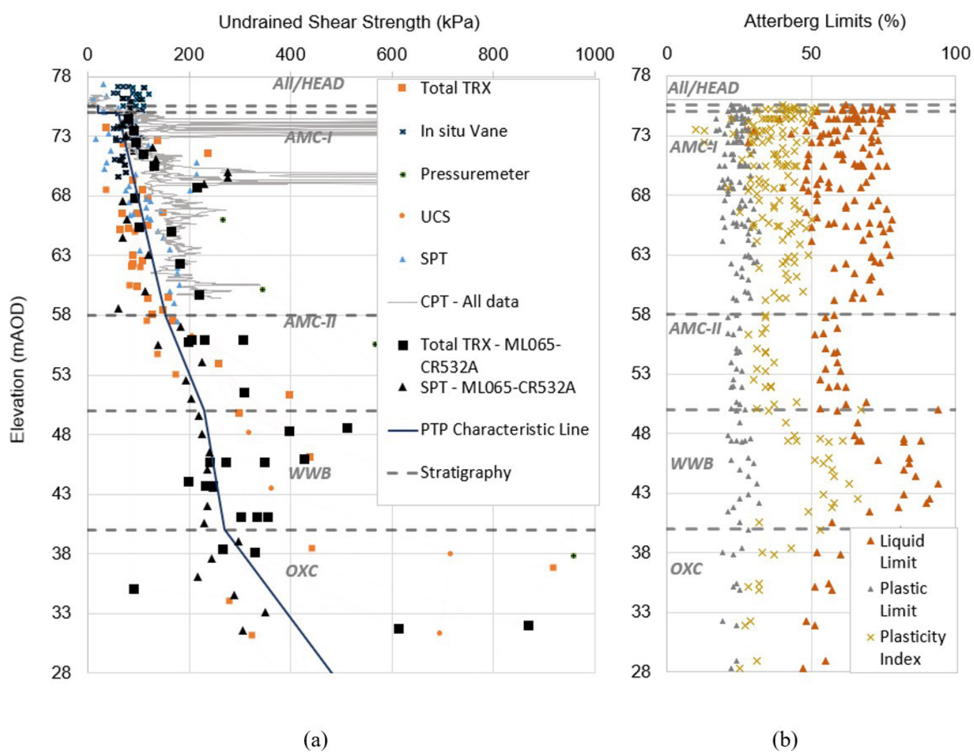

Figure 3. Undrained shear strength (a) and Atterberg limits (b) in the vicinity of the test site.

Table 2. Stratigraphy and Geotechnical Parameters assumed at the test site.

Geological unit	Top of layer (m AOD)	Thickness (m)	c_u (kPa)	*UCS* (MPa)
HEAD	75.6	0.6	20	-
AMC I	75	17	60+5.5z	-
AMC II	58	8	154+9.6z	-
WWB	50	10	230+4z	-
OXC	40	Not proven	-	0.54+0.035z

row of three 1500 mm diameter piles (same diameter as PTP10A) with a fixed pier providing longitudinal restraint. The fixed pier is connected to a 14x14x2 m deep pile cap, supported by nine 1800 mm diameter piles (same diameter as PTP11) in a 3x3 layout. The abutments are supported on six 1500 mm piles in a 3x2 layout. After completion of the test pile program, all working piles have been constructed as typical bored cast in-situ bored piles in the dry without the use of any support fluid.

3.2 Pile design

Pile design for the viaduct foundations has been carried out following the established standard practice in the UK. This corresponds to estimating unit shaft resistance in HEAD, AMC and WWB using the α design method, i.e. $f_s = \alpha c_u$ (Tomlinson & Woodward, 2008), where α is the empirical coefficient assumed as 0.5 and c_u is the undrained shear strength presented in Figure 3. A limit to $f_s = \alpha c_u$ of 125 kPa was applied to shaft resistance in clay. For the length of piles through OXC, the unit shaft resistance has been estimated using the approach proposed by Horvath & Kenney (1979), i.e. $f_s = 0.225\sqrt{UCS}$. A limit to f_s of 300 kPa has been applied to the design.

The unit base resistance in the OXC has been estimated as $f_b = 4.5\ UCS$, (Rowe & Armitage, 1984) where UCS is taken at the pile toe level. Table 3 presents the estimated ultimate resistance of the two test piles.

4. Test piles

4.1 Description of tests

As shown in Figure 4, the instrumentation in the two piles included 4 pairs of extensometers and 9 sets of strain gauges. The displacements of the top plate, toe and pile head and expansion of the O-cell were also measured electronically using Linear Voltage Displacement Transducers (LVDT).

The 1500 mm test pile, PTP10A, was installed with length of 41.06 m, incorporating the O-cell assembly at 36.1 m below the pile head. The maximum sustained gross load applied to the pile was 10.75 MN in each direction. At the maximum sustained load, the displacements above and below the O-cell assembly were 6.01 mm and 7.97 mm, respectively. At the next load increment with a gross applied load of 11.70 MN in each direction, the upper pile section above the O-cell was unable to sustain the applied load, see Figure 5.

Table 3. Estimated Ultimate Resistance of the test piles.

Test Pile ID (diam.)	Pile length (m)	Shaft capacity (MN)	Base capacity (MN)	Total capacity (MN)
PTP10A (1.5m)	41.06	17.8	5.7	23.5
PTP11 (1.8m)	39.05	19.2	7.4	26.6

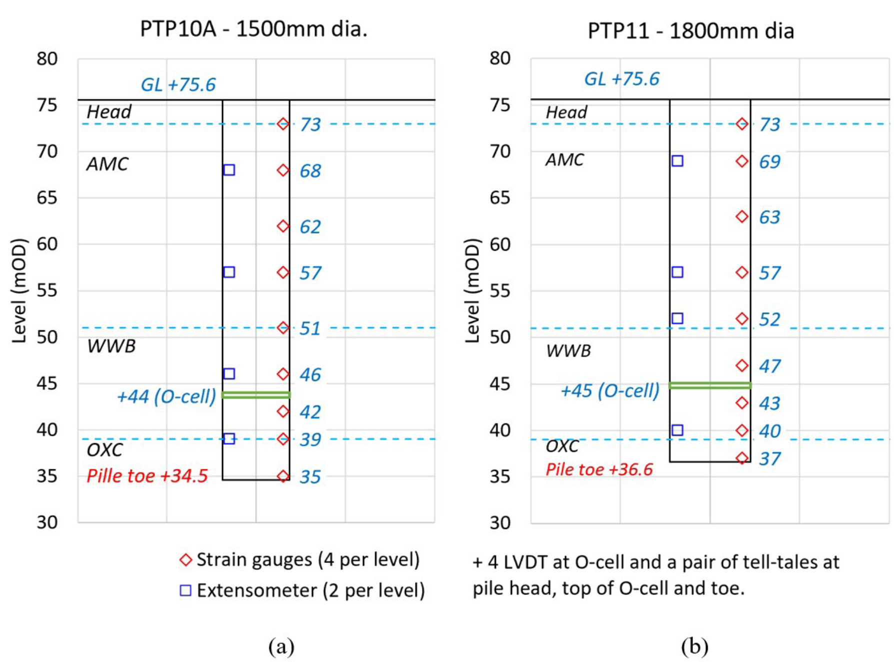

Figure 4. Schematic representation of the instrumentation in the test piles PTP10A (a) and PTP11 (b).

The 1800 mm test pile PTP11 was installed with length of 39.05 m, incorporating the O-cell assembly at 30.6 m below the pile head. The maximum sustained gross load applied to the pile was 13.32 MN in each direction. At this maximum sustained load, the displacements above and below the O-cell assembly were 4.97 mm and 10.13 mm, respectively. Again, the upper pile section was unable to sustain the applied load at the next load increment, see Figure 5.

4.2 Interpretation of the results

The load distribution along the pile shaft is shown in Figure 6 and has been calculated by multiplying the average strain at each level of strain gauges by the calculated axial stiffness (EA=71000 MN for PTP10A and EA=97800 MN for PTP 11). The strain gauges immediately above and below the O-cell (SG3 and SG4 in PTP10A, and SG3 in PTP11) recorded results that were inconsistent with typical load distribution patterns observed in test piles. These readings were excluded from the interpretation, as their close proximity to the O-cell may have caused anomalous strain measurements - likely due to high stress concentrations or reduced local concrete stiffness resulting from placement irregularities during tremie concreting around the O-cell assembly.

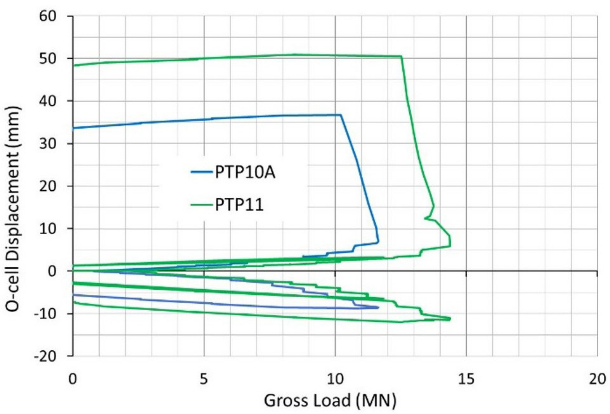

Figure 5. Upper and lower shaft movements.

The interpreted unit shaft friction between levels of strain gauges is summarised in Table 4.

The equivalent top load-displacement has been analysed using two methods, the CEMSET Analysis method (Fleming, 1992) and the conventional Equivalent Top Load (ETL) method (England, 2008). The CEMSET method was used to determine the behaviour of the pile above and below the O-cell by considering the upward and downward movement analysed separately. Figure 7 presents the individual CEMSET curves that produce the best fit load-displacement profiles with the measured test data, using the input parameters in Table 5. Given that both piles failed upwards, the base capacity has not been fully mobilised, therefore this base capacity has been estimated using the approach presented in Section 3.2 but slightly adjusted to fit the data for the downward movement curves of the two test piles.

Figure 8 shows the equivalent top-loading curves for the two test piles determined by combining the upward and downward load-displacement using the CEMSET method (dashed lines). It also shows and the equivalent top-loading

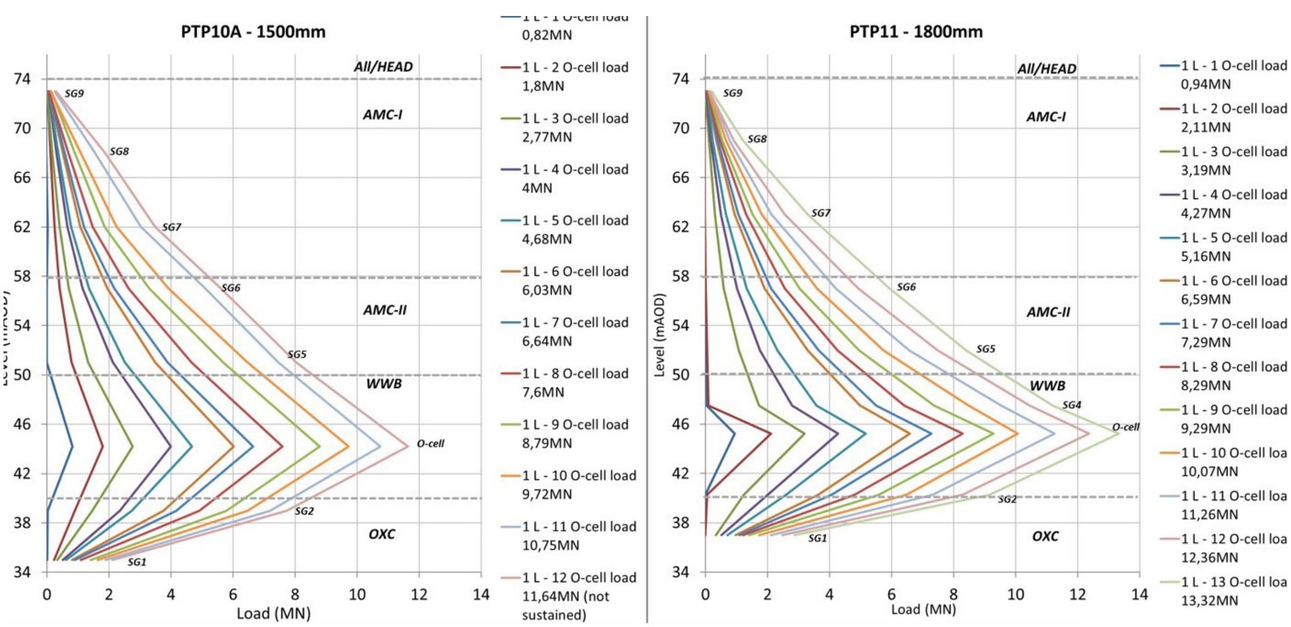

(a) (b)

Figure 6. Axial load calculated along the test piles PTP10A (a) and PTP11 (b).

Table 4. Interpreted unit shaft friction.

Levels (m AOD)	Strata	Unit shaft friction (kPa)	
		PTP10A	PTP11
75.6 - 73	HEAD	20	13
73 - 68.5	AMC	56	45
68 - 62.5		52	61
62 - 57		89	78
57 - 51.5		83	88
51 - 46	WWB	103	128
45 - 40		145	149
39 - 35	OXC	281	338

Table 5. Summary of input parameters for CEMSET analysis above and below the O-cell.

Input Parameter	PTP10A		PTP11	
	Above O-cell	Below O-cell	Above O-cell	Below O-cell
Q_s[1] (MN)	11.6	9.47	14.38	11.32
M_s (-)	0.0003	0.0004	0.0002	0.0006
Q_b[2] (MN)	-	5.0	-	6.5
E_b (MPa)	-	129	-	188
L_f (m)	31.6	9.46	30.6	9.46
K_e (-)	0.3	0.5	0.3	0.5
E_c (GPa)	40	40	40	40

[1]Ultimate shaft capacity. [2]Ultimate base capacity.

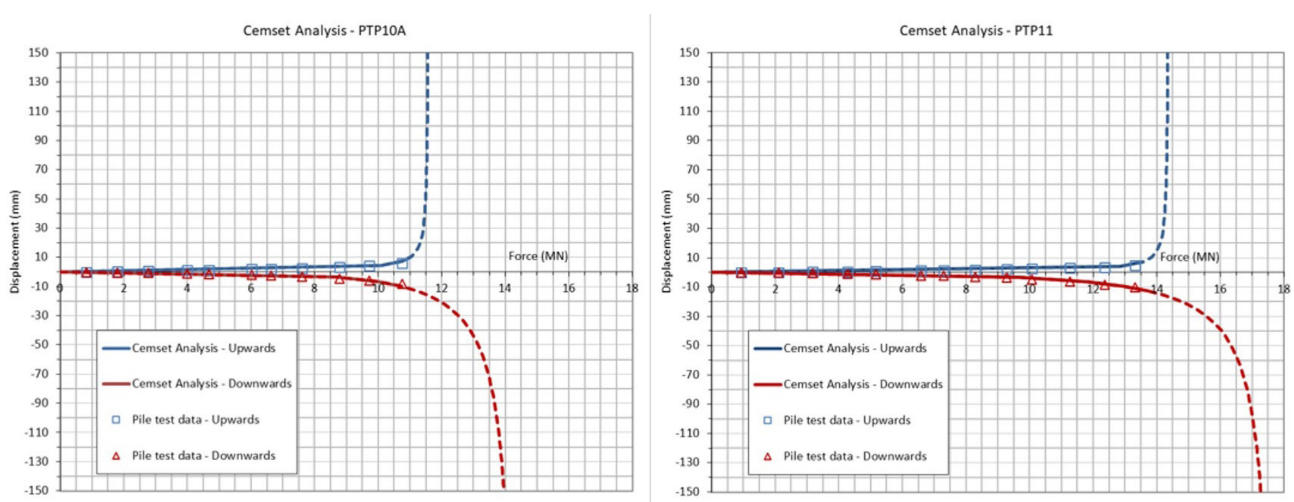

(a) (b)

Figure 7. CEMSET Analysis used to produce the best fit load-displacement profiles to the measured test pile data of PTP10A (a) and PTP11 (b).

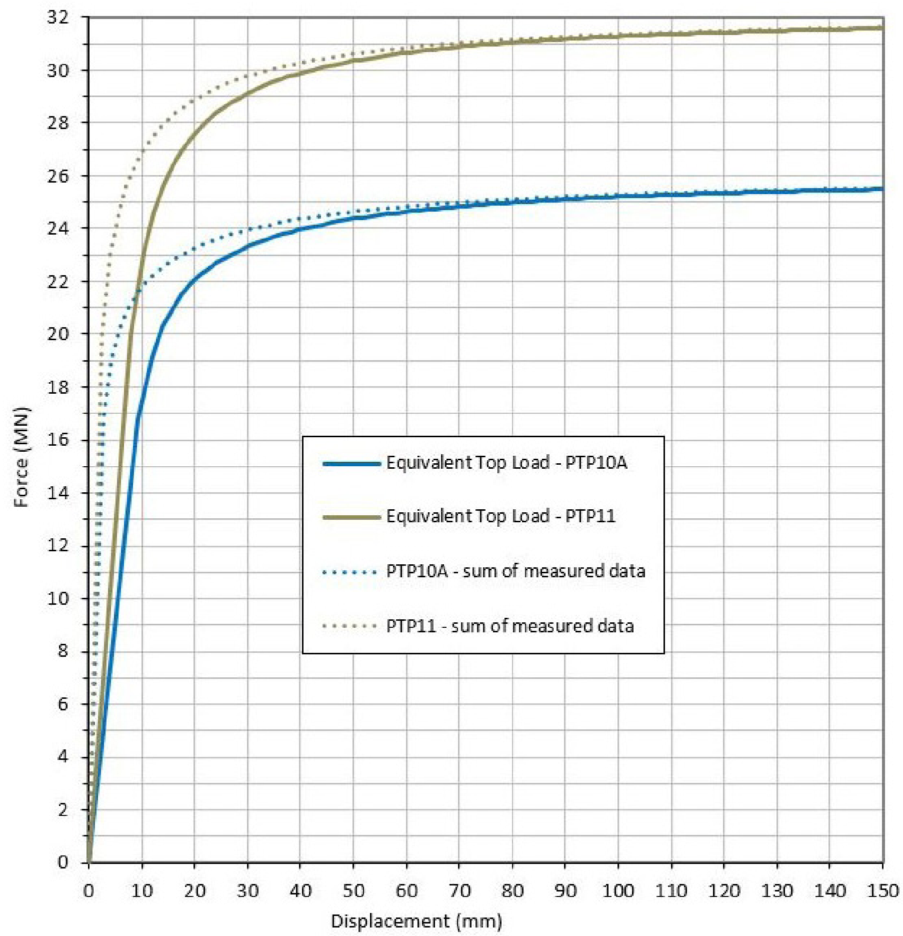

Figure 8. Equivalent top load displacement curves determined using CEMSET Analysis.

Table 6. Summary of estimated pile capacities.

Pile	Ultimate Capacity (MN)	
	Estimated in Section 3.2	CEMSET Analysis
PTP10A	23.5 (Q_s = 17.8; Q_b = 5.7)	26 (Q_s = 21.0; Q_b = 5.0)
PTP11	26.6 (Q_s = 19.2; Q_b = 7.4)	32 (Q_s = 25.5; Q_b = 6.5)

Q_s = Ultimate shaft capacity; Q_b = Ultimate base capacity.

curves corrected for the additional elastic shortening using the method proposed by England, 2009 (solid line).

Alternatively, the equivalent top-loading displacement curve has been approximated with the conventional ETL method. For this method, arbitrary displacement points were picked (1 mm, 2 mm, 3 mm, 4 mm, 5 mm, etc.) and the corresponding O-cell loads in the upwards and downwards curves have been measured at the selected displacement points. To take advantage of the fact that the test produced downward movement data, an extrapolation of the upward movement has been made for PTP10A and PTP11 using a suitable hyperbolic curve fitting the test data that corresponds to a high correlation coefficient ($R^2 > 0.99$). Figure 9 shows the ETL method (also corrected for the elastic shortening for top loaded piles) compared with the CEMSET method. The figure shows a good agreement between the two methods up until the point when extrapolation is introduced, where ETL method predicts a much stiffer response suggesting that the extrapolation using the ETL method may be unconservative in predicting the ultimate capacity of the pile. Table 6 shows the comparison of ultimate capacities between the design approach presented in Section 3.2 and those calculated from the CEMSET analysis.

4.3 Comparison with viaduct design

Figure 10 shows a good agreement between the unit shaft friction estimated using the design profile and the values

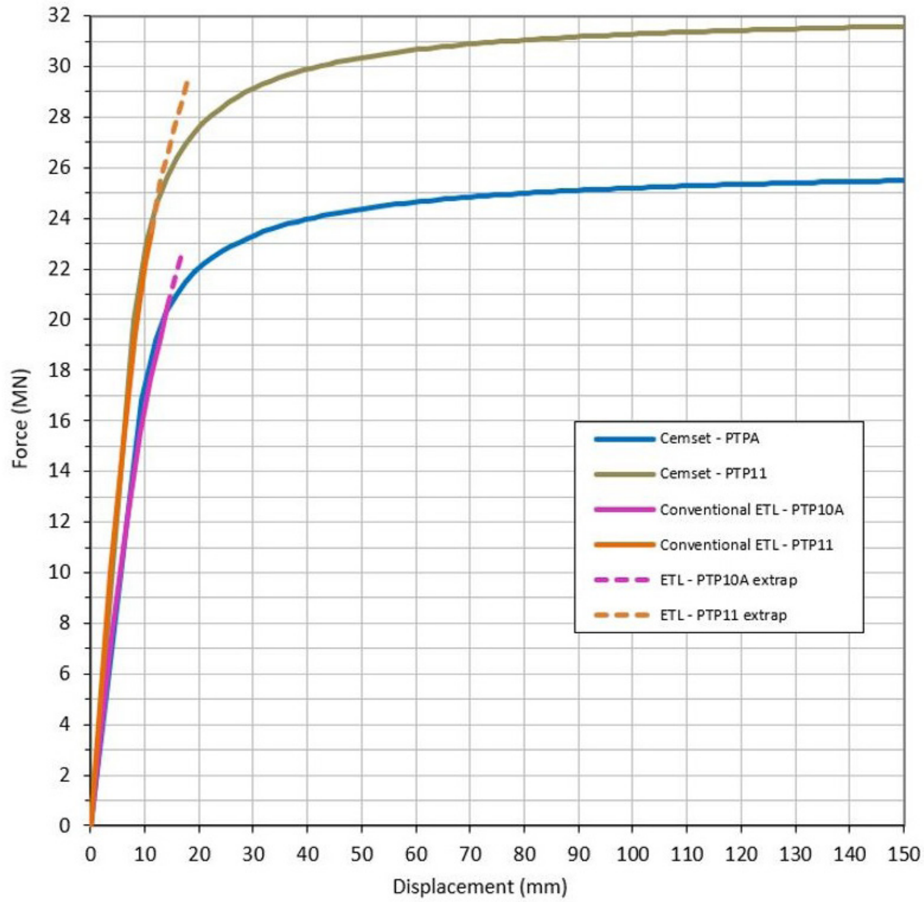

Figure 9. Comparison of equivalent top load displacement curves determined using CEMSET and ETL methods.

interpreted from the test pile data in most strata except the OXC where there is significant underprediction of the shaft resistance.

Particularly throughout AMC-I, the estimation of unit shaft friction based on design profile is slightly lower than interpretation of the test data, as expected given the slightly cautious undrained shear strength profile for the site-specific borehole data. There is no such trend for the AMC-II stratum except it is fair to assume the design values are in good agreement with the measured ones. The interpretation of the test data suggests constant unit skin friction between levels 52 and 62 m AOD, which is unlikely to be a correct representation since gradual increase in soil strength is expected. In WWB, the estimation based on design profile is slightly lower than interpretation of the test data for the bottom half of this unit, because a limit to $f_s = \alpha c_u$ of 125 kPa has been applied to shaft resistance in clay, otherwise a good agreement should be expected. It could be argued that such limit could be higher, for instance a limit to $f_s = \alpha c_u$ of 150 kPa could be recommended, however the current limit is only applicable to the unit shaft friction over a short length and therefore does not affect the overall pile capacity. In OXC it becomes clear that the assumed unit shaft friction based on design profile underestimated actual shaft resistance. This is possibly due to the assumption of a conservative characteristic strength in the Mudstone layer that resulted from the wide scatter in the available ground investigation data. While this is not demonstrated by Figure 10, it is also possible that the base capacity in OXC is being underestimated if the characteristic base parameters are conservative. However, noting that both piles only penetrated a short length into OXC and that more data should be considered to confidently infer any conclusions, it is considered prudent to keep the current approach in the viaduct pile design.

4.4 Analysis using 3D finite element analysis

The preliminary test piles were back-analysed using Plaxis 3D finite element (FE) program to mimic the measured performance of the test results under the bi-directional O-cell test before the introduction of load at pile head to derive the equivalent top loaded pile response. Although an axisymmetric 2D model would suffice, the decision to adopt

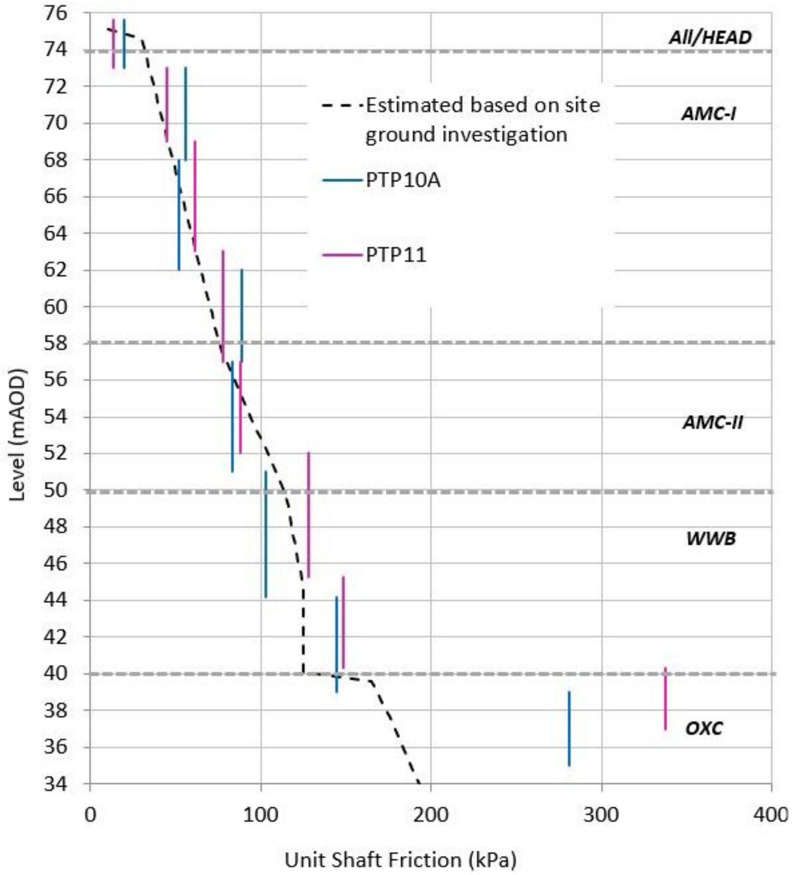

Figure 10. Comparison of unit shaft friction determined by preliminary test piles and design.

a full 3D model allows the assessment of lateral response of the pile be it as a single pile or as a pile group for the design of the viaduct foundations.

4.4.1 Methodology

In the FE model, the test pile was modelled by splitting the shaft into several sections to mimic the positions of the strain gauges installed to measure the load transfers during the test. Each of these shaft sections is then assigned a shear strength parameter to reflect the measured unit skin friction values, see Figure 11. Under the test load, the measured displacements of the O-cell's top and bottom plates, pile head and pile toe were compared and calibrated before the pile is loaded from the top.

It is worth noting that when assigning individual shear strength using interface element, only Plaxis command codes were used to change the input shear strength parameters rapidly for multiple assessments to calibrate the load-displacement of the test pile. The use of automated Python script would speed up this calibration process, but this is not used at this stage.

Apart from the shear strength parameters assigned to the test pile, soil properties of the ground and stiffness of the pile concrete are the other two variables which could affect the behaviour of the pile under the applied load. For the calibration undertaken, the following are the soil model and properties used in the FE model:

- concrete stiffness: 40-45 GPa;
- stiffness of the soils: E_u/c_u = 500-750.

Linear elastic perfectly plastic Mohr-Coulomb (MC) soil model has been used to represent the soils. Although parameters for more complex or advanced soil models are currently not available in this type of soils, an attempt is also made to calibrate one of the test pile using Small Strain Hardening Soil model (HSS) in Plaxis with a view to understand the significance of varying the type of soil model on the result of the back analysis. The parameters of the HSS have been based on the back analyses work undertaken for retaining walls in London Clay (Yeow, 2022) where the derived HSS parameters were found to be similar to the retaining wall back analyses with a Eu/cu ratio of approximately 1000 (Yeow, 2022). Although it is well understood the vertical stiffness of sedimentary deposits such as London Clay is usually lower than lateral stiffness (Gasparre, 2005), the same set of retaining walls back analysed parameters are first used to determine the behaviour of the 1500 mm diameter test pile before a more rigorous calibration is undertaken.

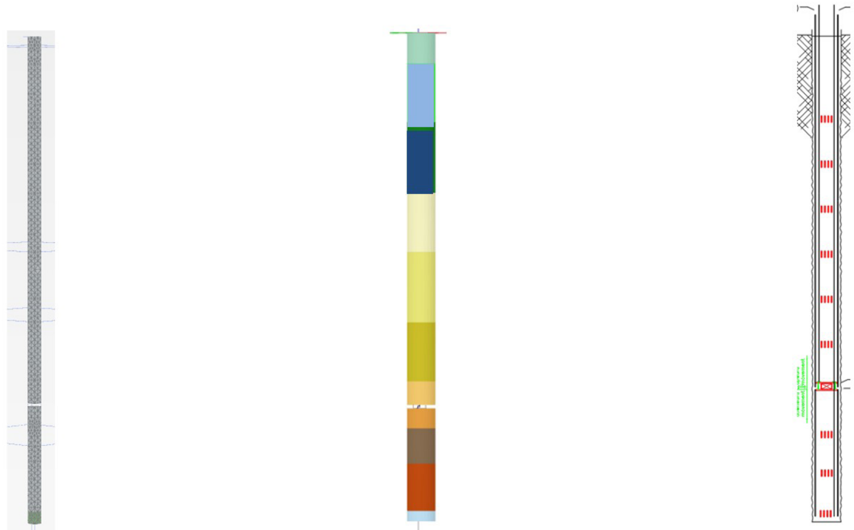

(a) model pile (b) interface with different shear strength (c) test pile instruments

Figure 11. Pile shaft with different shear strength values.

4.4.2 Test pile calibration using Mohr Coulomb soil model

The process of calibration started with the first set of parameters based on the pile design approach indicated in Section 3.2 to derive the unit shaft friction of the pile. Due to the low unit shaft friction in the OXC, the lower section of the pile settled excessively beyond a test load of 8MN for PTP10A. Similar observation for PTP11 albeit with slightly higher applied O-cell load.

With the derived unit shaft resistance from the test piles, the load displacement profiles for both the test piles are shown in Figure 12.

When load is applied from pile head, the equivalent load-displacement profiles are shown in Figure 13, including the range of response computed using MC soil model with different soil stiffness values. When comparing this to the CEMSET back-analysis, the difference in load-settlement performance of the piles at serviceability limit state is negligible although the ultimate capacity of the larger 1.8 m diameter test pile is approximately 5% lower. This could be due to more pronounced pile base softening effects on the larger test pile.

4.4.3 Further assessments using HSS soil model

In order to use the HSS model, the first task is to ensure the inherent undrained shear strength of the soil is comparable. Figure 14 shows comparison of the equivalent undrained shear strength of the soil derived using the retaining wall's HSS model with the characteristic profile presented in Figure 3.

With higher stiffness values based on the retaining wall parameters, the computed O-cell equivalent load displacement behaviour is presented in Figure 15. With this set of parameters, the upwards displacement of the test pile is showing stiffer response while the downwards displacement matches the measurement well.

It is also a rule of thumb that Eu/cu ratio of 500 (Katsigiannis, 2017) is used for displacement assessment of London Clay under vertical load. When the stiffness values in the HSS model is reduced to 50% of the values used for retaining walls, the following load displacement behaviour is computed and shown in Figure 16. With this set of stiffness parameters, both the computed upwards and downwards displacements show reasonable match with the measured values.

From the above comparisons using both the MC and HSS soil models, it is clear that as long as the strength parameters are correctly assigned, the ultimate capacity of the pile could be reasonably predicted. In the UK, piles are designed with an overall factor of safety of approximately 2.8. For PTP10A, the working load would be approximately 8.5 MN. The differences in stiffness values would affect the upwards displacement of the O-cell more than the downwards displacement. Such differences in stiffness would not affect the serviceability limit performance of the pile which is generally related to load-displacement up to 1.5 times the working load, or less than 13 MN for PTP10A, before the displacement exceeds the non-linear region or elasto-plastic behaviour of the pile. In this case the elasto-plastic behaviour initiates when the equivalent top load of greater than 16 MN.

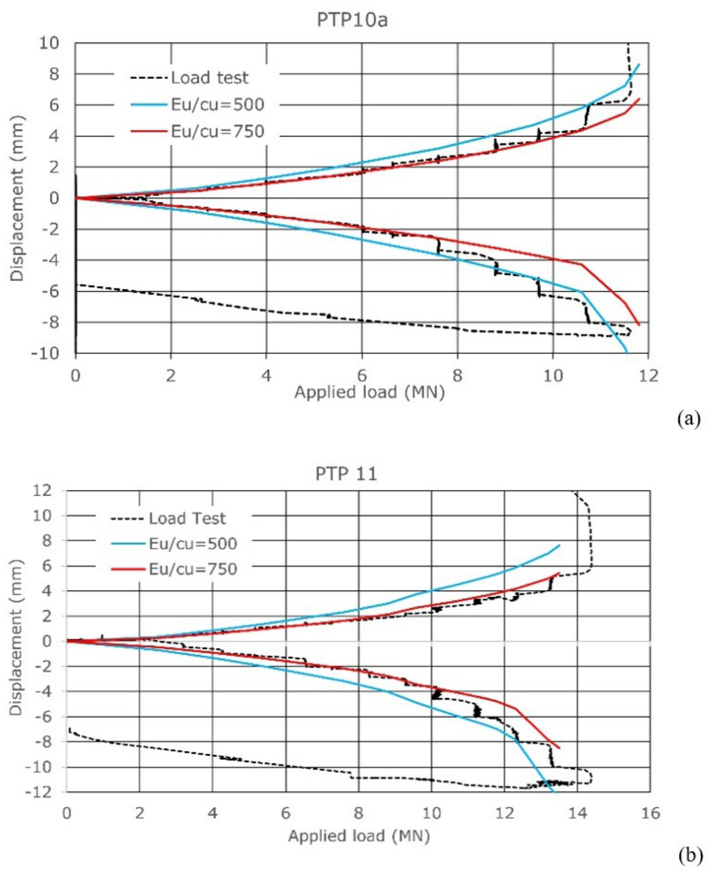

Figure 12. Load-displacement profiles for the test piles PTP10A (a) and PTP11 (b) back-analysed using Plaxis 3D model.

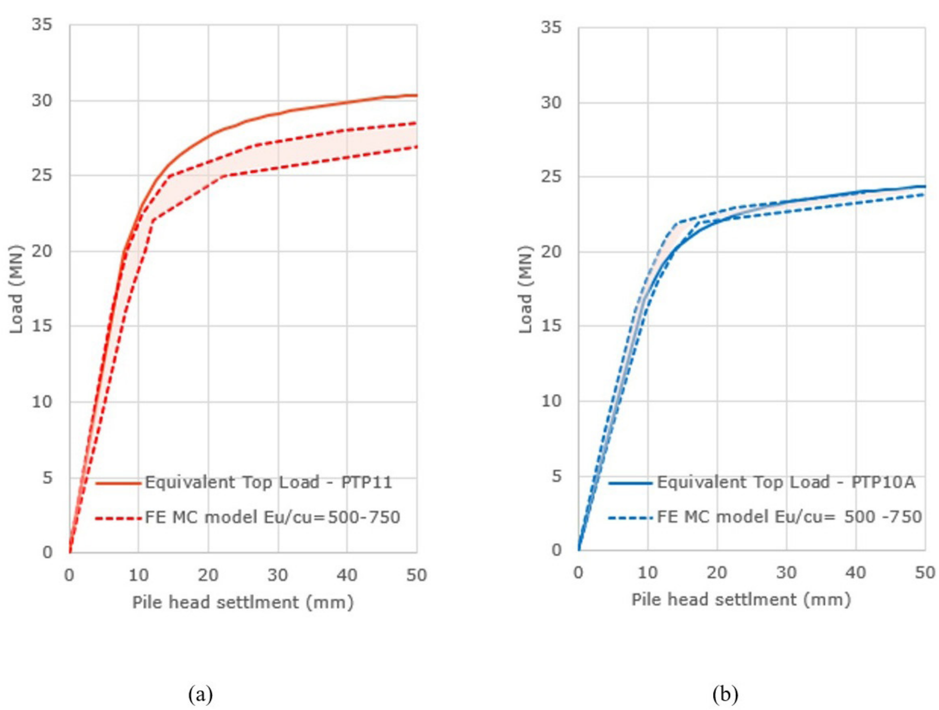

Figure 13. Range of load-displacement profiles for the test piles PTP10A (a) and PTP11 (b) with different Eu/cu ratios.

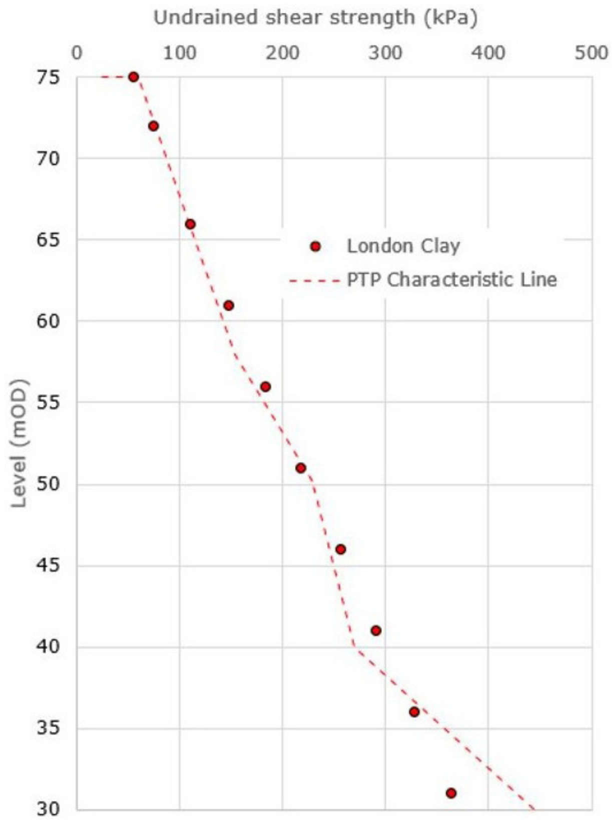

Figure 14. Equivalent undrained shear strength of the HSS model compared to PTP characteristic profile.

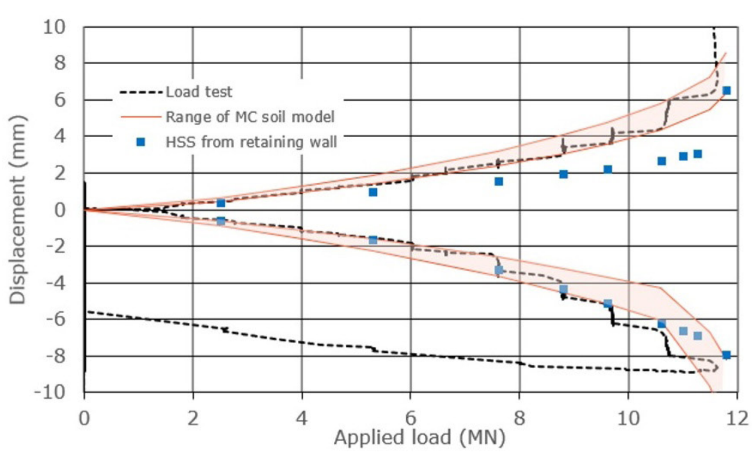

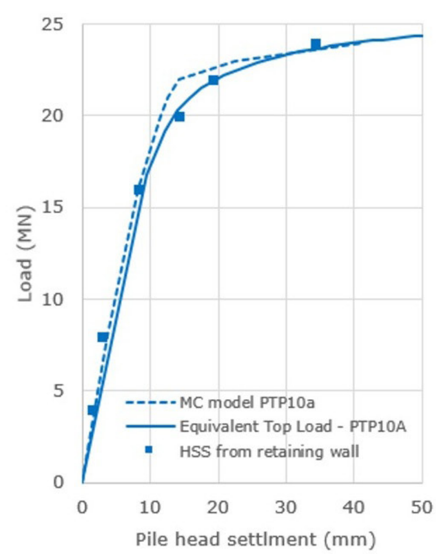

(a) (b)

Figure 15. Computed load displacement of PTP10A using retaining wall HSS model. (a) applied load versus upwards and downwards displacement; (b) Pile head settlement versus load.

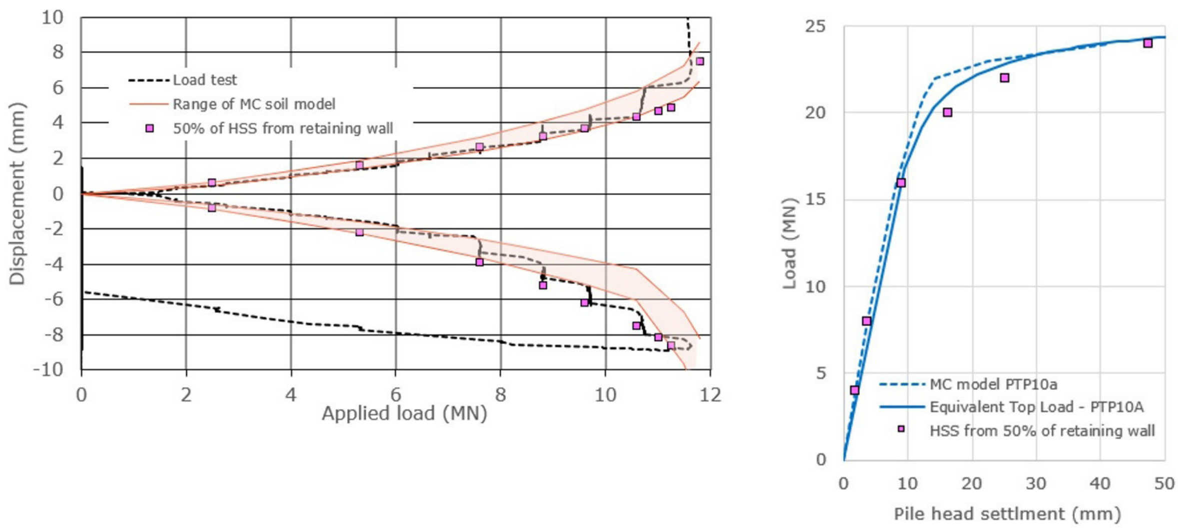

(a) (b)

Figure 16. Computed load displacement of PTP10A using 50% of stiffness of retaining wall HSS model. (a) applied load versus upwards and downwards displacement; (b) pile head settlement versus load.

5. Conclusions

The ultimate pile capacities estimated using the approach assumed by the designer outlined in Section 3.2 were calculated as 23.5 MN and 26.6 MN for test piles PTP10A and PTP11, respectively. In this approach the unit shaft resistance in HEAD, AMC and WWB was calculated as $f_s = 0.5c_u$, while through OXC, calculated as $f_s = 0.225\sqrt{UCS}$. The unit base resistance has been estimated as $f_b = 4.5UCS$, although base capacity has not been fully mobilised. This methodology was validated through the interpretation of pile load test results, confirming it as the recommended approach for the succession of clay and mudstone formations within the Ancholme Group.

When this approach is compared with the back-analysed unit shaft frictions from the test pile data, there was a good agreement in the clay layers but it underestimated the shaft resistance in the Mudstone layers. It is possible that the assumption of characteristic strength of the Mudstone layer is conservative. More ground investigation data and pile test in these strata would be required to verify a more appropriate strength parameters in order to incorporate higher shaft resistance values.

Due to the short length of pile in the OXC, where the most discrepancy in the shaft resistance value was found, the design approach presented for pile design in AMC/WWB/OXC is considered appropriate and slightly conservative for pile lengths between 39 and 41 m.

The back-analysis of the two preliminary test piles in Plaxis 3D finite element models using linear elastic perfectly plastic Mohr-Coulomb and Small Strain Hardening Soil models has confirmed the load-settlement characteristic necessary to verify the performance of the pile under serviceability limit state, which is generally related to load-displacement up to 1.5 times the working load. The assessment has also shown that differences in stiffness would not affect the serviceability limit performance of the piles and that, as long as the strength parameters are correctly assigned, the ultimate capacity of the piles could be reasonably predicted.

The back-analysis presented in this paper demonstrates that standard UK pile design practices are adequate for the ground conditions encountered (Ancholm Group). This outcome reflects a successful collaboration between design teams and contractors to outline a scope of test piles, enabling an efficient and verified design solution for the 880m-long Thame Valley Viaduct.

Acknowledgements

The Authors would like to express their gratitude to HS2 and EKFB for their permission to use and publish the test pile data included in this paper and share the lessons learnt from designing and interpreting such valuable test results with fellow practitioners designing bored cast in-situ pile in similar ground conditions.

Declaration of interest

The authors have no conflicts of interest to declare. All co-authors have observed and affirmed the contents of the paper and there is no financial interest to report.

Authors' contributions

Sergio Vitorino: conceptualization, data curation, formal analysis, investigation, methodology, project administration, resources, software, supervision, validation, visualization, writing – original draft. writing – review & editing. Hoe-Chian Yeow: conceptualization, data curation, formal analysis, investigation, methodology, resources, software, supervision, validation, visualization, writing – original draft. writing – review & editing.

Data availability

The datasets generated analyzed in the course of the current study are available from the corresponding author upon request. All data produced or examined in the course of the current study are included in this article. The pile test data generated and analysed in the course of the current study are not publicly available due on-going project where the data is sourced.

Declaration of use of generative artificial intelligence

This work was not prepared with any assistance of generative artificial intelligence (GenAI).

List of symbols and abbreviations

c_u	undrained shear strength
f_1	CPT and SPT correlation constant
fs	unit shaft friction in kPa
m AOD	metre Above Ordnance Datum
q_c	cone resistance
z	depth below top of stratum
E_b	soil modulus as base
E_c	concrete Young's Modulus
K_e	CEMSET parameter: centroid of friction transfer
L_f	CEMSET parameter: length of pile
M_s	CEMSET parameter: shaft flexibility factor
N_{kt}	cone correlation constant
Q_b	base resistance
Q_s	shaft resistance
UCS	unconfined compressive strength
α	empirical correlation constant used for pile design in cohesive soils
σ_v	vertical stress

References

Clayton, C.R.I (1995). *The standard penetration test (SPT): methods and use (R143)* (144 p.). London: CIRIA.

England, M.G. (2008), Review of methods of analysis of test results from bi-directional static load tests. In W. F. van Impe & P. O. van Impe (Eds.), *Deep foundations on bored and augered piles* (pp. 235-239). London: Taylor & Francis Group.

Fleming, W.G.K. (1992). A new method for single pile settlement prediction and analysis. *Geotechnique*, 42(3), 411-425. http://doi.org/10.1680/geot.1992.42.3.411.

Gasparre, A. (2005). *Advanced laboratory characterisation of London clay* [Doctoral thesis]. Imperial College London, London.

Hayes, J.A. (November/December, 2012). The landmark of Osterberg Cell Test. *Deep Foundation*.

Horvath, R.G., & Kenney, T.C. (1979). Shaft resistance in rock socketed drilled piers. In *Proceedings of the symposium on deep foundations* (pp. 182-214). Reston: ASCE.

Institution of Civil Engineers – ICE. (2017). *ICE specification for piling and embedded retaining walls* (3rd ed.). London. http://doi.org/10.1680/icesperw.61576.

Katsigiannis, G. (2017). *Modern geotechnical codes of practice and new design challenges using numerical methods for support excavations* [Doctoral thesis]. University College London, London.

Rowe, R.K., & Armitage, H.H. (1984). *The design of piles socketed in weak rock* (Report GEOT-11-84, 365 p.). London, ON: University of Western Ontario.

Tomlinson, M.J., & Woodward, J. (2008). *Pile design and construction prac*tice (5th ed.). London: Taylor & Francis.

Yeow, H.C. (2022), Case histories of deep excavation and limit states design in accordance with Eurocode 7 using advanced soil model. In *Proceeding of the 20th International Conference of Soil Mechanics and Geotechnical Engineering*, Sydney, Australia.